analytical chemistry

Article

pubs.acs.org/ac

Kinetic Rate Determination via Electrophoresis along a Varying Cross-Section Microchannel

Monica A. Kapil, Yuchen Pan, Todd A. Duncombe, and Amy E. Herr*

Bioengineering, University of California, Berkeley, California 94706, United States

Supporting Information

ABSTRACT: High throughput, efficient, and readily adoptable analytical tools for the validation and selection of reliable antibody reagents would impact the life sciences, clinical chemistry, and clinical medicine. To directly quantify antibody−antigen association and dissociation rate constants, k_{on} and k_{off}, in a single experiment, we introduce a microfluidic free-standing kinetic polyacrylamide gel electrophoresis (*fs*KPAGE) assay. Here, an antibody is immobilized in zones along the length of a single freestanding polyacrylamide gel lane of varying cross-sectional width. Fluorescently labeled antigen is electrophoresed through each immobilized antibody zone, with local cross-sectional area determining the local electric field strength and, thus, the local interaction time between immobilized antibody and electromigrating antigen. Upon crossing, the interaction yields immobilized immunocomplex. The k_{on} is quantified by assessing the amount of immunocomplex formed at each interaction time. To quantify k_{off}, immobilized zones of fluorescently labeled immunocomplex are subjected to a buffer dilution and monitored over time. We determine k_{on} and k_{off} for prostate-specific antigen (PSA) and make a comparison to gold-standard values. The *fs*KPAGE assay determines k_{on} and k_{off} in a single experiment of less than 20 min, using 45 ng of often limited antibody material and standard laboratory equipment. We see the *fs*KPAGE assay as forming the basis for rapid, quantitative antibody-screening tools.

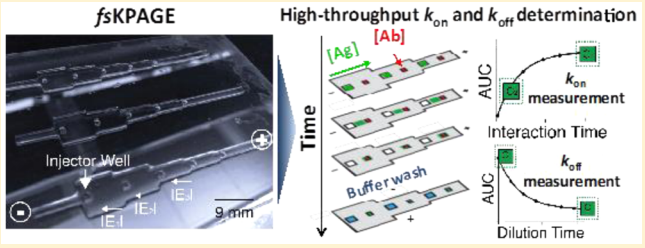

Used in a wide-range of immunoassays[1,2] and therapeutics,[3,4] over a million antibodies are estimated to be in production. Nevertheless, for immunoreagents, false positives (nonspecific binding), false negatives (low specificity), and reproducibility (lot-to-lot, vendor variability) remain problematic. Compounding the challenge is a lack of consensus on methods for the selection of antibody reagents.[5,6] While validation assays and rigor vary, the dissociation constant, K_d, provides insight into specificity and suitable applications. The K_d describes the dynamic equilibrium between the dissociation (unbinding) and association (binding) kinetic rate constants ($K_d = k_{off}/k_{on}$) for a specific antibody−antigen pair. Both enzyme linked immunosorbent assay (ELISA) and surface plasmon resonance (SPR) do not provide k_{off} and k_{on} independently, due to mass transport limitations affecting each assay.[7] Independent assessment of the k_{on} and k_{off} is not commonly performed. Yet, two antibodies with identical K_d values can have dramatically different binding kinetics, making performance for a specific application difficult to predict from the K_d value alone. Hence, both k_{on} and k_{off} values would aid validation and selection of immunoreagents for specific applications.[8,9]

In previous work, we demonstrated a method called kinetic polyacrylamide gel electrophoresis (KPAGE) to make kinetic measurements via electrophoresis along glass microchannels filled with polyacrylamide gels.[10] That KPAGE assay reports k_{on} by monitoring immobile immunocomplex formed as a plug of fluorescently labeled antigen is electrophoresed through a zone of immobilized antibody. Formation of immunocomplex is measured across a range of antibody−antigen interaction times, with interaction time controlled by the velocity of the electromigrating antigen zone as determined by the strength of the applied electric field and the electrophoretic mobility of the species. In microchannel-based KPAGE, the k_{on} was determined from a sequence of end point measurements presenting throughput limitations.

To overcome these throughput limitations, we introduce here a free-standing kinetic polyacrylamide gel electrophoresis (*fs*KPAGE) device that supports concurrent measurement of a range of protein−antibody interaction times. To control the range of antibody−antigen interaction times, now in one experiment and in one device, we use a single microfluidic "gel lane" with controlled and varied cross-sectional area (Figure 1). Each of the 6 regions has a unique and fixed cross-sectional area, with each region housing two features: (i) one antigen injection reservoir and (ii) one immobilized antibody zone. In each region, the local antigen−antibody interaction time is determined by the local cross-sectional area of the channel and, thus, the local electric field strength (which determines the local electrophoretic velocity of the antigen peak migrating through that region). To determine k_{off}, buffer is electrophoresed over immobilized immunocomplex while dissociation is monitored. To design for adoption, the *fs*KPAGE device uses a form factor

Received: November 24, 2015
Accepted: March 10, 2016

DOI: 10.1021/acs.analchem.5b04445
Anal. Chem. XXXX, XXX, XXX−XXX

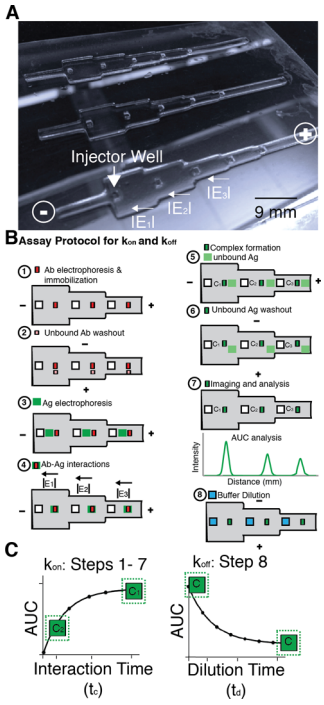

Figure 1. Free standing kinetic polyacrylamide gel electrophoresis (*fs*KPAGE) enables rapid, quantitative measurements of antibody–antigen (Ab–Ag) binding kinetics. (A) Image of the *fs*KPAGE device fabricated using photopatterning of a polyacrylamide gel "lane". The gel lane has 6 regions, each with a distinct cross-sectional area, loading well, and immobilized antibody zone. When an electric potential is applied using one electrode at each end of the lane, the local electric field is determined by the width of the region. (B) An 8-step protocol allows determination of k_{on} and k_{off} for an antigen–antibody pair. Step 1: Antibody patterning; a solution of Ab is pipetted into each injection well and then electrophoresed down the lane. The gel contains a photoactive monomer, such that brief UV exposure results in covalent attachment of the Ab peak to the gel and creation of a stationary Ab zone (toward the back of each injection well). Step 2: Excess, unbound Ab is electrophoresed out of the gel. Step 3: An Ag solution is loaded into each injection well and electrophoresed along the axis of the gel lane. Step 4: Electromigrating Ag peaks interact with cognate stationary Ab zone in each of the 6 distinct regions, yielding 6 distinct interaction times (t_c) dictated by the local electric field (E_1–E_6). Steps 5 and 6: Immunocomplex forms and excess Ag is electrophoresed off of the gel in the transverse direction. Step 7: The gel is imaged and quantification of immunocomplex is performed via AUC analysis. The amount of immunocomplex formed is proportional to the t_c. Step 8: To determine the k_{off}, buffer is electrophoresed over stationary immunocomplex for a set dilution time (t_d), while the time-dependent decay in immunocomplex signal is monitored.

matching standard liquid handling tools (96-well format) and operation is controlled by a single electrode pair. The *fs*KPAGE assay presents a complementary avenue for quantitative characterization of immunoreagents at the point of use, a topic that has garnered substantial interest from clinicians, researchers, and manufacturers of immunoreagents,[11] as well as institutions that both publish and fund research.[12−16]

MATERIALS AND METHODS

Apparatus and Imaging. To quantify immunocomplex formation, fluorescence images were collected using an inverted epi-fluorescence microscope equipped with CCD camera, filter cubes, and an automated *x*–*y* stage as well. Large area imaging was performed with a scan slide function controlled by Metamorph software (Molecular Devices, Sunnyvale, CA). A 2× objective (PlanApo, N.A. = 0.08, Olympus, Center Valley, PA) with a CCD exposure time of 100 ms was used. To assess the electrophoretic mobility of the antigen peaks, images were collected using a ChemiDoc XRS Universal Hood II (Bio-Rad, Hercules, CA). Custom-macros were developed and image analysis was conducted using ImageJ software (NIH, Bethesda, MD). Intensity plots were extracted by selecting a region of interest (ROI) along the axial dimension of each gel region. Postprocessing used in-house algorithms implemented with MATLAB (R2014a, MathWorks, Natick, MA). A Tecan Infinite microplate reader (Mannedorf, Switzerland) was used for fluorescence immunoassay equilibrium experiments. The height of the *fs*KPAGE device was measured by a MicroXAM-100 Optical Profilometer (ADE phase Shift, Tucson, AZ). A protocol to estimate the temperature of the *fs*KPAGE structures was devised to measure Joule heating effects during electrophoresis. A noncontact infrared (IR) thermometer with laser targeting (Westward 2ZB46) was selected to dynamically assess temperature. An alignment study was done to ensure that the noncontact area sensed was confined to the *fs*KPAGE structures (see Supporting Information). The IR thermometer has a distance-to-spot ratio (D/S) of 9:1 (per manufacturer's specifications). The sensor was positioned ∼30 mm away from the surface of the gel to yield a sensing spot size of ∼3 mm. Using surfaces of known temperature, it was verified that sensing occurs at the center of the thermometer detector unit and is offset by 26 mm from the laser pointer on the thermometer. With this in mind, the center of the sensor was vertically aligned with the top of the gel structure for all measurements to ensure that the measured area was limited to the confines of the *fs*KPAGE structure.

Reagents. Solutions of 30% (w/v) (29:1) acrylamide/bis(acrylamide) were purchased from Sigma-Aldrich (St. Louis, MO). The photoinitiator 2,2-azobis[2-methyl-*N*-(2-hydroxyethyl) propionamide] (VA-086) was purchased from Wako Chemical (Richmond, VA). GelBond PAG film and Gel Slick glass plate coating were purchased from Lonza (Base, Switzerland). Photomasks were designed using AutoCAD 2013 (Autodesk, Inc., San Rafael, CA) and printed on Mylar transparencies at CAD/Art Services (Brandon, OR). 10× Tris-glycine native electrophoresis buffer (25 mM Tris, 192 mM glycine, pH 8.3) was purchased from Bio-Rad. Benzophenone methacrylamide monomer (BPMA, (*N*-[3-[(4-benzoylphenyl)-formamido]propyl] methacrylamide) was synthesized and characterized by PharamAgra Laboratories Inc. (Brevard, NC). Stocks of BMPA at 100 mM in dimethyl sulfoxide (DMSO) were stored at −20 °C until use. Proteins and antibodies were fluorescently labeled in-house using Alexa Fluor 488 and 568 protein labeling kits (Invitrogen) and purified by Bio-Gel columns (Bio-Rad Laboratories). Purified prostate specific antigen (PSA) and anti-prostate specific antigen antibody were purchased from Abcam. Alexa Fluor 568 goat anti-mouse IgG (H+L) antibody was purchased from Life Technologies Corporation.

ELISA-Like Fluorescence Immunoassay Equilibrium Constants. Immunoassay-based equilibrium experiments were conducted in white, opaque 96-well microplates (Thermo Fisher Scientific Inc., Waltham, MA). The microplate was incubated with 70 μL of 0.01 nM PSA monoclonal antibody labeled in Alexa Fluor 568 for 2 h at room temperature on an Orbitron shaker. The microplate was then washed 3 times using

DOI: 10.1021/acs.analchem.5b04445
Anal. Chem. XXXX, XXX, XXX–XXX

1× Tris-glycine and subsequently incubated with blocking buffer (1× Tris-glycine and 1% bovine serum albumin, BSA) for 2 h to prevent nonspecific binding. Unbound BSA was then washed out of each well using 3 washes with 1× Tris-glycine buffer. 70 μL volumes of PSA labeled with Alexa Fluor 488 were added to each well in concentrations of 0.009−20 nM (n = 3 for each concentration) and incubated at room temperature for 1 h. Each microplate housed one row of wells for blank wells, one row of wells containing just antibody solution, and one row of wells containing PSA incubated at the maximum and minimum concentrations. The microplates were imaged using a fluorescence microplate reader after PSA antibody immobilization on the plate and again after PSA incubation. Equilibrium constants (K_d) were determined by quantifying the amount of PSA bound at 50% for the range of concentrations stated above. Dissociation rate constants were quantified by determining the amount of PSA unbound after three 1 h dilutions. Association rate constants were calculated from the measured K_d and k_{off} values.

Fabrication and Operation of *fs*KPAGE Devices. The *fs*KPAGE devices were fabricated via UV photopatterning[17] using a precursor solution containing 6% T acrylamide (w/v), 3.3% C bis-acrylamide cross-linker (w/w), 0.5% VA-086 photoinitiator (w/v), and 2.5 mM BMPA. Prior to UV exposure, the precursor solution was degassed for 5 min under house vacuum with sonication. For *fs*KPAGE device fabrication, a borosilicate glass substrate sandwiched a photomask with a surface-functionalized polymer sheet (GelBond, a commercially available transparent, flexible polyester film). Two spacers with a predefined thickness were aligned on two sides of the GelBond film (spacers from C.B.S. Scientific, MVS-0508R: Mini-Vertical Gel Wrap Spacer Set, 0.5 mm thick × 8 cm, Del Mar, CA). Another glass plate was seated on top of the spacers. The precursor solution was pipetted into the ∼500 μm gap between the GelBond and the glass cover and then exposed to UV light through a 390 nm long pass filter to prevent BMPA activation (Edmund Optics, Barrington, NJ). The intensity of UV and UV exposure times were optimized for 6% T monomer concentration with 0.5% VA-086, the water-soluble azo-initiator, at 30 mW/cm^2 and 600 s exposure (measured by OAI 308 UV intensity meter, OAI, San Jose, CA). After UV exposure, the polymerized *fs*KPAGE devices were gently washed with deionized water to remove unpolymerized monomer. After photopatterning, the *fs*KPAGE devices were soaked in run buffer for 15 min on an Orbitron shaker. When removed, a Rainin P2 pipet tip was connected to the house vacuum and applied to each well to remove residual unpolymerized monomer or excess run buffer. The *fs*KPAGE device was seated in a custom manifold for imaging and buffer wash steps (see Figure S-1). Two electrode wicks wetted with run buffer were aligned on top of both ends of the gel and placed in contact with graphite electrodes. Sample solution was pipetted into the sample wells at a volume of 0.5 μL, and the two electrodes were connected to an external high-voltage power supply (Power-Pac HV; Bio-Rad Laboratories).

Protocol for *fs*KPAGE Determination of Binding Kinetics. To conduct the *fs*KPAGE assays, a 0.5 μL volume of antibody (Ab) solution at 425 nM concentration was pipetted into each injection well and electrophoretically injected into each channel region with an applied voltage of 855 V for 60 s (Step 1, Figure 1B). Covalent attachment of Ab to the BPMA cross-linked into the polyacrylamide gel occurred through UV exposure via the ChemiDoc Universal Hood II. The gel was exposed to flood UV (350−365 nm) light with the gel facing the UV source and then immersed in buffer for 6 min (Figure S-2). After UV exposure, unbound Ab was electrophoresed across the width of the gel until the peak migrated out of the gel lane (Step 2, Figure 1B). Next, 0.5 μL of antigen (Ag) (5.65 μM) was electrophoretically injected from each loading well into the abutting channel region via an applied voltage of 855 V for 30−60 s (Step 3 of Figure 1B). The local width of each channel region controlled the local electric field and, hence, the local velocity of each Ag band and interaction time (t_c).

Using the described *fs*KPAGE structures and applied potentials, we scrutinized interaction times spanning 10 s < t_c < 60 s (Step 4, Figure 1B) at six distinct t_c values with three to six replicates each. Real-time fluorescence imaging of the entire device was performed using the ChemiDoc imager for monitoring of immunocomplex formation and Ab−Ag interaction times for each channel region. Unbound Ag was electrophoretically washed off in the transverse channel direction (Step 5−6, Figure 1B). The gel was subsequently imaged using an epi-fluorescence microscope, and the amount of immunocomplex formed for each t_c was quantified via area under the curve (AUC) analysis. Determination of k_{off} was performed by electrophoresing buffer in the transverse channel direction, diluting the immunocomplex formed in steps 1−5 during a set dilution time (t_d). In this step, the time-dependent decay of the immunocomplex signal allows determination of k_{off}. Here, immunocomplex was subjected to buffer dilution for a dilution time (t_d) from 0 to 120 min and monitored via epi-fluorescence imaging. See Table S1 for the voltage protocol used in all *fs*KPAGE steps.

Estimation of Interaction Time, t_c. For k_{on} measurements, we define the t_c as the time required for a plug of Ag to traverse a zone of immobilized Ab. The interaction time was then determined by computing the electrophoretic velocity of the Ag (u_{Ag}) divided by the width of the antigen plug (w_{Ag}) migrating through the immobilized antibody zone, where $t_c = \frac{W_{Ag}}{U_{Ag}}$.

Estimation of Kinetic Rate Constants k_{on} and k_{off}. Epi-fluorescence micrographs of the immunocomplex signals for each t_c and t_d were fit to Gaussian distributions and AUC determined by integrating the distribution (see Supporting Information for the fitting method). For k_{on} and k_{off}, the AUC for each immunocomplex concentration was computed for each t_c and t_d. Controls for nonspecific binding were performed with non-UV exposed gels, UV exposed gels, and gels with nonspecific antibody present. We employ a Langmuir one-to-one antibody-to-antigen binding model,[8] as monoclonal antibody purification is known to result in protein unfolding, mis-folding, and aggregation that may yield only one active binding site.[18,19] Experimental data were fit to a 3-parameter binding curve fit model derived from binding association and dissociation expressions to extract kinetic rates.[20] For each kinetic rate, multiple *fs*KPAGE experiments where preformed and curve fit to extract kinetic rates for both k_{on} and k_{off}. We assumed that the rates extracted were normally distributed and the mean, standard deviation, and standard error of the mean were computed (n = 3−5 for each rate). We report error in the final kinetic rate constants as 1.96 standard deviations from the mean (1.96× standard error of the mean) or 95% of the area of the normal distribution. The error in the immunocomplex peak AUC was computed in a similar manner.

DOI: 10.1021/acs.analchem.5b04445
Anal. Chem. XXXX, XXX, XXX−XXX

RESULTS AND DISCUSSION

Principles of Operation for the *fs*KPAGE Assay. To determine antigen−antibody binding kinetic rates in a single experiment, we sought to control antibody−antigen interaction times in a one-step assay. To accomplish this, we employed a free-standing gel "lane" of ever reducing cross-sectional area (step changes), one injector well and one immobilized antibody zone in each region of uniform cross-section, and one electrode pair for the entire device. A plug of fluorescently labeled antigen was then electrophoresed from each injection well, through the cognate immobilized antibody zone with the local cross-sectional area determining the local electric field strength, E. The electrophoretic velocity of the migrating antigen peak, U_{Ag}, depends on the electrophoretic mobility of the antigen, μ_{Ag}, and the local electric field, E, where

$$U_{Ag} = E\mu_{Ag} \quad (1)$$

and the duration of the interaction between the electromigrating antigen and immobilized antibody zone is defined as

$$t_c = \frac{4\sigma_{Ag}}{E\mu_{Ag}} \quad (2)$$

where t_c depends on $4\sigma_{Ag}$ (the width of the antigen peak) and the local E. We design the assay with a form factor compatible with conventional laboratory liquid handling technologies (e.g., hand-held multichannel pipettes, automated robotic fluid delivery systems). The lengths of each cross-sectional region and well-to-well distances match spacing on 96 well-plates. Eight distinct regions with distinct cross-sectional area are implemented in series, yielding up to 8 immunocomplex studies in a single experiment. Up to 12 concurrent experiments are feasible in the device footprint described.

With the length of each channel region constrained, we studied how the cross-sectional area (width) and associated local electrical resistance affects the local E for a given applied voltage (V). The resistance is defined as $R = \rho L/A$ where ρ is the electrical resistivity of the buffer, L is the total channel length, and A is the cross sectional area (i.e., $A = w \times H$, where w is the local channel width; H is the channel height). Both L and H are fixed in each region of uniform cross-sectional area; thus, E is dependent on w (as defined by Ohm's Law) where V = current (I) × R:

$$E = V/L = IR/L = I\rho/(wH) \quad (3)$$

The *fs*KPAGE assay requires t_c values ranging above and below equilibrium times;[10] thus, assuming typical low and intermediate binding rate kinetics for antigen−antibody binding pairs, the requirement translates into an operational specification of 10 s < τ_{eq} < 20 s. For a given applied voltage, we design the *fs*KPAGE channel widths to be in the range of 3 mm ≤ w ≤ 8 mm. To precisely define the width of each immobilized antibody zone, we use a photopatterning technique. The polyacrylamide gel comprising the *fs*KPAGE structure includes a benzophenone methacrylamide monomer in the polyacrylamide matrix.[21−23] This photoactive molecule abstracts hydrogen from C−H bonds from surrounding species upon brief exposure to UV light, thus resulting in covalent immobilization of a zone of injected antibody to the polyacrylamide gel.

To validate the *fs*KPAGE assay, we calculated and experimentally determined t_c for a PSA antigen and antibody pair and then compared the values with analytical results (Figure 2). As a model, we employed a monoclonal PSA antibody and a PSA[24] antigen with a measured $\mu_{EP} = 6.8 \times 10^{-5}$ cm^2 V^{-1} s^{-1}. Depending on the applied voltage, ranging from 50 to 200 V, the interaction times were in the range of 6 s ≤ t_c ≤ 60 s with a corresponding 50 V/cm ≤ E ≤ 300 V/cm (Figure S-3). To assess uniformity of the local E distribution in this two-dimensional geometry, we performed numerical simulations that suggest acceptably uniform E distributions in both the transverse and axial channel dimensions, as is critical to the control of Ab−Ag interaction times (Figure S-4)

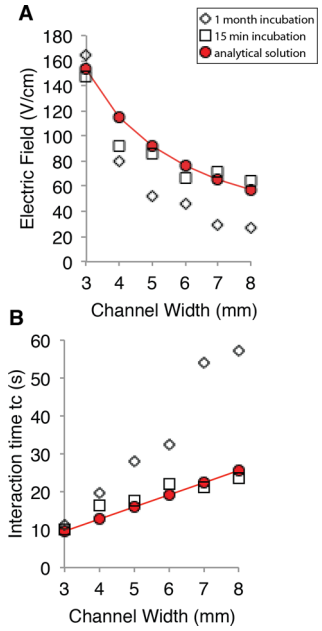

Figure 2. Geometry dictates local electric field strength and electrophoretically determined interaction times. Analytical solutions of the local electric field strength and interaction times were computed and compared to experimental values from gels stored at two different storage conditions to determine the stability of the assay. In Condition 1, gels were stored in 1X Tris-glycine for 1 month in an aluminum foil covered petri dish at 4°C, and in Condition 2, gels were incubated in fresh 1X Tris-glycine for 15 min prior to use. Experimental estimates of the local electric field strength were made using the measured electrophoretic velocity of tracer proteins and calibrated electrophoretic mobilities. The width of each gel lane is inversely proportional to the local electric field strength.

Storage Conditions and Impact on Operation of the Open Format *fs*KPAGE Structures. Owing to the open design of the *fs*KPAGE device, we assessed device and assay stability during storage and during operation. Thus, in a first consideration regarding assay stability, we characterized the impact of gel storage conditions on *fs*KPAGE assay performance. We selected two storage conditions: In Condition 1, gels were stored in 1× Tris-glycine for 1 month in an aluminum foil covered Petri dish at 4 °C, and in Condition 2, gels were incubated in fresh 1× Tris-glycine for 15 min prior to use (Figure 2). Under Condition 1, greater variation and ∼50% lower t_c values were observed for 10 s ≤ t_c ≤ 60 s than for gels stored per Condition 2. We further observed that Condition 1 yielded t_c and E values that differed by 50% from calculations of each, based on geometry and a given V. In contrast, under storage Condition 2, we observed <10% differences in t_c from those calculated on the basis of geometry for a given V. We attribute the observed performance differences under storage Condition 1 to increased ionic strength in the gels, owing to buffer evaporation during storage. We measured the local

DOI: 10.1021/acs.analchem.5b04445
Anal. Chem. XXXX, XXX, XXX−XXX

conductivity of the buffer by varying the voltage (V) and measuring the current. Via the IV curve, we estimated the electrical resistivity from the slope of the curve and calculated the conductivity. We observed increases of conductivity (~50%) during electrophoresis within 10 days of storage. As the ionic strength increases, the Debye length and mobility decrease, thus slowing interaction times as compared to ideal values and possibly corroborating our experimental observations.

Thermal Behavior of the Open Format *fs*KPAGE Structures. In a second consideration regarding stability during operation, the open gel format sees Joule heating balanced by heat loss by convection ($\dot{q}_{conv}$) and evaporation ($\dot{q}_{evap}$) to ambient conditions. The thermal considerations are described by

$$E^2\sigma_g H = \dot{q}_{conv} + \dot{q}_{evap} \quad (4)$$

Heat generation due to Joule heating depends on E, the electrical conductivity of the *fs*KPAGE media (σ_g), and the height of the gel (H). Langmuir's evaporation model and the Antoine Equation[25] describing the temperature−vapor pressure relationship, eq 4, can be recast as

$$E^2\sigma_g H = C_c(T_{gel} - T_{env}) + \Delta H_{Vap}(P_v - P_p)\sqrt{\frac{m}{2\pi R T_{gel}}} \quad (5)$$

where C_c is the heat transfer coefficient, T_{gel} and T_{env} are the temperature of the gel and surrounding environment, respectively, ΔH_{Vap} is the enthalpy of vaporization, P_v and P_p are the vapor pressure of liquid water and partial pressure of water vapor in air (at room temperature), m is the vapor molecular mass, and R is the ideal gas constant.

We first compared the expected Joule heating-induced temperature rise in the widest and narrowest regions of the *fs*KPAGE device (i.e., 8 and 3 mm wide gel regions) where the local E is at the lowest and highest strength, respectively. Changes in T_{gel} are expected to perturb intermolecular binding forces that drive association or dissociation.[26] We measured both the temperature and height of each *fs*KPAGE gel region after 60 and 120 s of electrophoresis time and also analytically solved for the local temperature using eq 5 (Figure 3). The estimated gel temperature (T_{gel}) in the 8 mm wide region of the *fs*KPAGE device matched experimental results with a 0.5% difference in value. The estimated T_{gel} in the 3 mm wide region differs from measured values by 45% (Table S-2). We attribute the difference between the predicted and measured T_{gel} in the 3 mm wide region of the device to difficulty in accurately measuring the partial pressure of water vapor in air. Joule heating increases the gel temperature and accelerates the evaporation process (from 19 to 42.4 °C), which makes the moisture environment directly above the gel difficult to determine. Therefore, for this back-of-the-envelope estimate, we extracted an estimated partial pressure of water vapor in air value from empirical saturation pressure−temperature data and employed that value in our calculations.[27]

Evaporation-induced changes in gel height, h, are expected to affect the ionic strength of the *fs*KPAGE media. Free ions can bind to charge groups on the antigen or antibody binding site on the epitopes or paratopes, obstructing combination.[28] Previous studies on red cell antibodies conjugated with anti-D Rho Immunoglobulin showed that reducing ionic strength from 0.17 to 0.03 M (6 fold decrease) increased the association

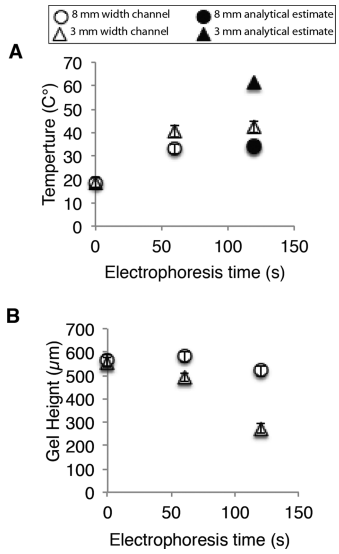

Figure 3. Temperature rise in *fs*KPAGE structures during electrophoresis. (A) Analytical and empirical estimates of the temperature in the gel lane during *fs*KPAGE operation. Analytical estimates differ from experimental results by 0.5% in the widest gel region and by 45% in the narrowest gel region. (B) Gel height does not notably decrease during the association rate measurements (~60 s). Gel height was measured using an optical profilometer.

rate constant 1000-fold.[29] Here, in analysis of PSA binding, we again considered the 3 and 8 mm wide regions of the *fs*KPAGE device, in which we observed gel height decreases measured using an optical profilometer (n = 3) during electrophoresis that yielded local ionic strength increases of 3% (0.047 M, 8 mm wide region) and 11% (0.051 M, 3 mm wide region) over the starting ionic strength (0.046 M) of the *fs*KPAGE media.

***fs*KPAGE Determination of Association Kinetic Rate Constant, k_{on}.** Next, to determine k_{on} for a PSA and monoclonal antibody pair, we applied *fs*KPAGE and first assessed nonspecific interactions at ambient conditions by measuring nonspecific signal in gels that had undergone different experimental conditions. Three different cases were considered; in the first case (Case 1), PSA was electrophoresed into a gel that had not been exposed to UV; in Case 2, PSA was injected into a UV exposed gel, and in Case 3, zones of off-target antibody were immobilized and PSA was subsequently injected. All of these cases were then compared to signal from immobilized on-target PSA antibody (Case 4). Here, we measured a nonspecific signal of 1.5 ± 0.2% for Case 1, 6.2 ± 1% for Case 2, and 6.5 ± 2% for Case 3. All cases were then compared to signal from immobilized on-target PSA antibody (Case 4), where we measured a 90% increase in immunocomplex signal in comparison to Cases 2 and 3.

The k_{on} for the PSA and monoclonal antibody pair was then determined (Figure 4). The use of *fs*KPAGE reported a k_{on} of $1.8 \times 10^4 \pm 0.19 \times 10^4$ M^{-1} s^{-1} (n = 3, using a new device for each measurement, Figure 4). The k_{on} was compared to literature SPR[24] values and in-house ELISA binding measurements, with computed association rates using the same buffer system used in the *fs*KPAGE. SPR reported a value of $4.1 \times 10^4 \pm 1.3 \times 10^4$ M^{-1} s^{-1} and ELISA resulted in a value of $2 \times 10^4 \pm 1.03 \times 10^4$ M^{-1} s^{-1}. For both SPR and ELISA, the *fs*KPAGE k_{on} for PSA is within an order of magnitude. However, both the SPR and ELISA measurements gave run-to-run variation of 81% and 85% higher than that of the *fs*KPAGE measurements,

DOI: 10.1021/acs.analchem.5b04445
Anal. Chem. XXXX, XXX, XXX−XXX

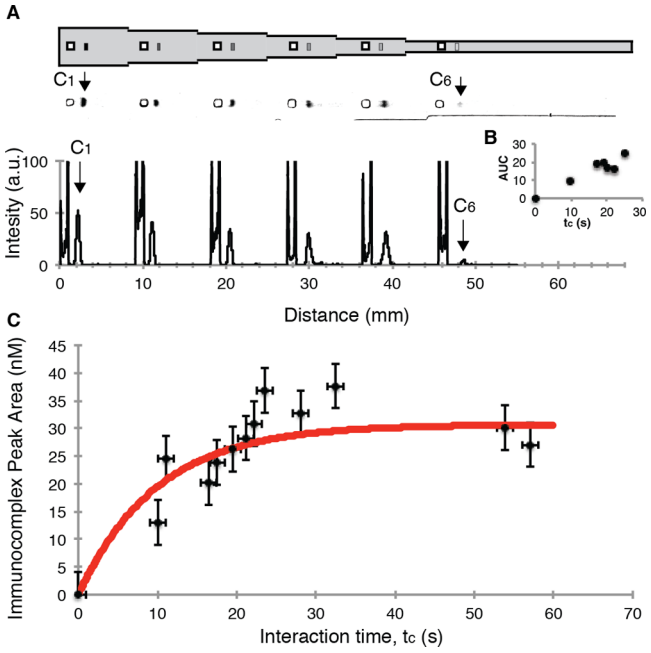

Figure 4. Direct determination of association rate constants with *fs*KPAGE. (A) Epi-fluorescence micrographs of immunocomplex signals formed after antigen (green fluorophore) has interacted with the immobilized antibody for a set interaction time, t_c. Intensity profiles of immunocomplex peaks at different interaction times ranging from 0 to 60 s are quantified and show that as t_c increases the AUC of the immunocomplex peaks (C_1 and C_6) increases (B). (C) Black circles represent *fs*KPAGE measurements of PSA immunocomplex at different t_c values. On-chip measurements of the association rate constant k_{on} was calculated from a 3-parameter binding curve fit model (red) and plotted against the measured PSA immunocomplex. Error bars are calculated from three replicate trials. k_{on} for the affinity interaction of PSA was $1.8 \times 10^4 \pm 0.19 \times 10^4$ M^{-1} s^{-1}.

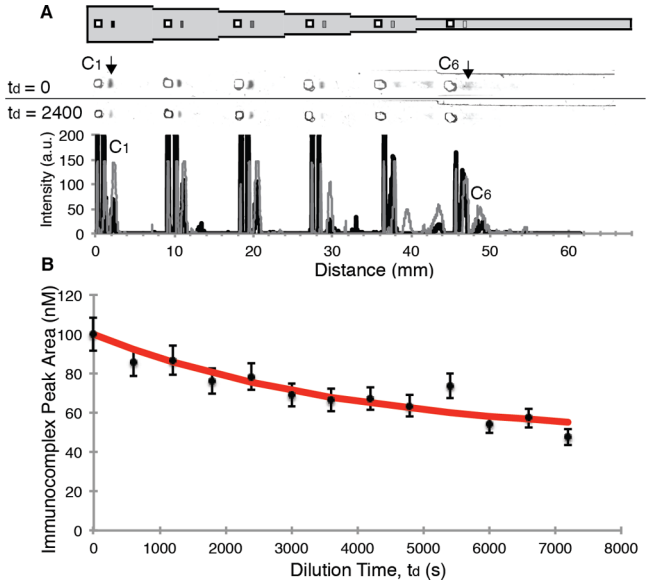

Figure 5. Direct determination of dissociation rate constants via *fs*KPAGE. (A) Epi-fluorescence micrograph time course of PSA immunocomplex dissociation (green fluorophore signal). Intensity profiles of immunocomplex peaks (C_1 and C_6) at different dilution times (t_d) points ranging from 0 to 7200 s are quantified. As t_d increases, the AUC of the immunocomplex peaks decreases. (B) Black circles represent *fs*KPAGE measurements of PSA immunocomplex at different t_d values. Measurements of the dissociation rate constant k_{off} were calculated from a 3-parameter binding curve fit model (red) and plotted against the measured PSA immunocomplex for each t_d. Error bars are calculated from replicate trials. k_{off} was determined to be $2.5 \times 10^{-4} \pm 2 \times 10^{-4}$ s^{-1}.

respectfully, thus suggesting *fs*KPAGE may be more reliable and robust than either technique.

***fs*KPAGE Determination of Dissociation Kinetic Rate Constant, k_{off}.** We applied *fs*KPAGE to measure the k_{off} of the PSA and monoclonal antibody pair, also at ambient room temperature conditions (Figure 5). We observed time-dependent dissociation of the immunocomplex, decreasing from 100% and asymptoting to 47% at the longest dissociation times studied (i.e., 7200 s or 2 h) (Figure 5B). The k_{off} measurement plateaus at an offset of 47%, as expected and commonly observed with antibody antigen pairs due to low dissociation rates.[30] For this PSA pair, a dilution time of ~9.3 h of continuous buffer dilution would be needed to fully dissociate to a baseline of 0% bound plus nonspecific binding. In practice, a minimum of 5% decrease in signal is needed to measure the dissociation.[20] In this case, we were well above the minimum standard. In regards to the binding kinetics, the *fs*KPAGE yielded k_{off} measurements of $2.5 \times 10^{-4} \pm 2 \times 10^{-4}$ s^{-1}. The dissociation constant K_d, computed from k_{off} and k_{on}, was 14 nM. Literature reports based on SPR[24] establish k_{off} for PSA as $4.5 \times 10^{-5} \pm 0.67 \times 10^{-5}$ s^{-1}. In our ELISAs, we determined $k_{off} = 3.0 \times 10^{-5} \pm 0.5 \times 10^{-5}$ s^{-1}. These k_{off} values allowed us to compute K_d = 1.86 and 1.54 nM via SPR and ELISA, respectively. The k_{off} from SPR and ELISA (pH 8.3) are both roughly an order of magnitude lower than the k_{off} determined by *fs*KPAGE and the same order of magnitude for the computed K_d. We hypothesize that differences in the measured dissociation rate values arise from the high electric field strengths needed for *fs*KPAGE (for long dilutions of up to 1−2 h). Joule heating can increase the local in-gel temperature, thus enhancing evaporation and binding dissociation. Thus, we next sought to understand the impact of local temperature on determination of binding kinetic rate constants using the *fs*KPAGE assay.

Mitigating Joule Heating Induced Temperature Rises for *fs*KPAGE Determination of k_{on} and k_{off}. To assess the temperature dependence of kinetic rate constants for this binding pair, we implemented the *fs*KPAGE assay in a cold room (4 °C) and compared it to *fs*KPAGE conducted at room temperature. Under the 4 °C conditions, the *fs*KPAGE assay reported $k_{on} = 5.2 \times 10^3 \pm 0.1 \times 10^3$ M^{-1} s^{-1} (n = 3), $k_{off} = 9.1 \times 10^{-3} \pm 0.11 \times 10^{-3}$ s^{-1} (n = 6), and K_d = 17.5 μM (Figure 6). Under the 4 °C conditions, the time needed for the PSA antigen−antibody pair to reach equilibrium was 3.5× longer than required under room temperature conditions. Even after 2 h of dilution at 4 °C, nearly 80% of the immunocomplex remained complexed (compared to 50% at room temperature). Both kinetic rate constants were observed to be an order of magnitude lower at 4 °C than at room temperature (Figure 6A,B), yielding a K_d that was 2 orders of magnitude higher at 4 °C.

The observed temperature-dependent binding behavior may be attributed to the fact that most antibody−antigen pairs that contain a carbohydrate on the binding epitope involve primary hydrogen bonds, which are known to be exothermic, and are more stable at lower temperatures.[31] Epitope mapping of PSA shows that the antigenic epitope contains a carbohydrate

DOI: 10.1021/acs.analchem.5b04445
Anal. Chem. XXXX, XXX, XXX−XXX

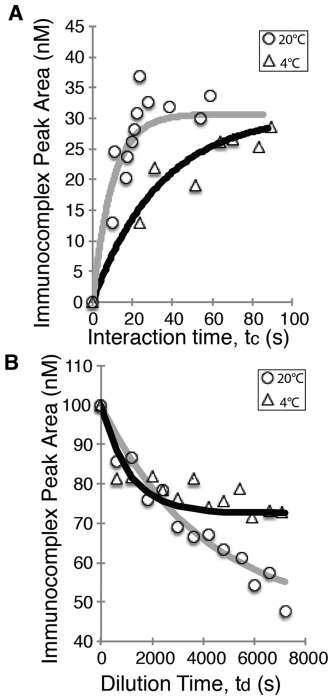

Figure 6. Association and dissociation rate constants measured at 4 °C decrease by an order of magnitude at cold room temperatures versus room temperature *fs*KPAGE. (A) The circles and triangles represent the association rate of *fs*KPAGE measurements of PSA immunocomplex measured at room temperature and at 4 °C and their corresponding curve fittings to the data represented by the gray and black curves. It takes 3.25× longer to reach equilibrium at 4 °C. On-chip measurements of the association rate constant k_{on} were calculated from a 3-parameter binding curve fit model (black and gray curves) that was plotted against the measured PSA immunocomplex. (B) The circles and triangles represent the dissociation rate of *fs*KPAGE measurements of PSA immunocomplex measured at room temperature and at 4 °C. On-chip measurements of the dissociation rate constant k_{off} were calculated from a 3-parameter binding curve fit model (black and gray curves) and plotted against the measured PSA immunocomplex.

moiety and forms noncovalent hydrogen bonds.[32,33] The characteristic aligns with our observation that PSA binding to antibody more readily dissociates at higher temperatures, due to the exothermic nature of hydrogen bonds, and thus exhibits higher dissociation rates. More broadly, binding pairs with identical K_d values have been observed to require 20× longer equilibrium times at 4 °C than at 37 °C,[34−36] suggesting that the association and dissociation kinetic rates are independently affected by temperature in a manner that may not be evident when considering the K_d alone. The observation further supports the assertion that direct measurement of both the association and dissociation kinetic rate constants yields important insight into binding characteristics across a range of temperatures.

CONCLUSIONS

Tremendous resources are routinely invested in choosing suitable immunoreagents for a specific application. Investment of resources into antibody production, for use as immunoreagents, is also significant. Quantitative assays for assessing immunoreagent performance, against a specific protein target, would be particularly useful to immunoassay developers, if available at the bench. As such, we report on the design, development, optimization, and characterization of *fs*KPAGE, a high-throughput, quantitative microfluidic-binding assay for direct quantification of kinetic rates in a single experiment. Importantly, the assay is designed to be easily adoptable, using standard biology lab equipment. The device comprises one long mesoscale gel channel with 6 distinct channel widths, thus passively varying the strength of the local electric field (using a single electrode pair). The local channel width dictates antigen velocity and, thus, antigen−antibody interaction times. Interaction times from 10 to 60 s were achieved, making the *fs*KPAGE assay suitable for a variety of binding pairs relevant to immunoassays. A thermal analysis of open *fs*KPAGE structures was performed, with empirical findings pointing to changes in gel height and temperature during operation, thus leading to studies where control of the ambient temperature during *fs*KPAGE was explored. The *fs*KPAGE assay provides a feasible means to realize rapid, quantitative, antibody screening in a single experiment at the bench. We see *fs*KPAGE as useful for assessing important but difficult-to-characterize interaction kinetics, especially for immunoassay developers who are interested in assessing the performance of a favored immunoreagent (i.e., with immunoreagent storage or lot-to-lot variation) to ensure final immunoassay quality over time.

ASSOCIATED CONTENT

Supporting Information

The Supporting Information is available free of charge on the ACS Publications website at DOI: 10.1021/acs.analchem.5b04445.

Photos of manifolds; protein capture optimization; voltage protocol for *fs*KPAGE assays; estimation of association constants k_{on} and k_{off}; analytical solutions of the local electric field and interaction times at different applied voltages; field strength throughout each distinct cross-sectional area in the *fs*KPAGE device; contributions to noncontact temperature readings from background temperature sources located outside the confines of *fs*KPAGE structures of known temperature; parameters used in analytical estimation of the temperature in gel and comparison to experimental results (PDF)

AUTHOR INFORMATION

Corresponding Author

*E-mail: aeh@berkeley.edu. Phone: 510-666-3396. Fax: 510-642-5835.

Notes

The authors declare no competing financial interest.

ACKNOWLEDGMENTS

The authors acknowledge members and alumni of the Herr Lab for helpful discussion and critical feedback, as well as the QB3 Biomolecular Nanofabrication Center (BNC) for infrastructure. M.A.K. and T.A.D. are National Science Foundation (NSF) Graduate Research Fellows. Y.P. is a fellow of the Kang Family Graduate Fellowship for Biotechnology. M.A.K. is a University of California Dissertation-Year Fellow. This work was supported by a National Science Foundation CAREER award (CBET-1056035 to A.E.H.). A.E.H. is an Alfred P. Sloan research fellow in chemistry.

DOI: 10.1021/acs.analchem.5b04445
Anal. Chem. XXXX, XXX, XXX−XXX

REFERENCES

(1) Sternberger, L. A.; Hardy, P. H.; Cuculis, J. J.; Meyer, H. G. *J. Histochem. Cytochem.* **1970**, *18*, 315−333.
(2) Berglund, L.; Björling, E.; Oksvold, P.; Fagerberg, L.; Asplund, A.; Szigyarto, C. A.-K.; Persson, A.; Ottosson, J.; Wernérus, H.; Nilsson, P.; et al. *Mol. Cell. Proteomics* **2008**, *7*, 2019−2027.
(3) Perchiacca, J. M.; Ladiwala, A. R. A.; Bhattacharya, M.; Tessier, P. M. *Proc. Natl. Acad. Sci. U. S. A.* **2012**, *109*, 84−89.
(4) Kariolis, M. S.; Kapur, S.; Cochran, J. R. *Curr. Opin. Biotechnol.* **2013**, *24*, 1072−1077.
(5) Collins, F. S.; Tabak, L. A. *Nature* **2014**, *505*, 612.
(6) Bradbury, A.; Plückthun, A. *Nature* **2015**, *518*, 27.
(7) Schuck, P.; Zhao, H. In *Surface Plasmon Resonance*; Springer: New York, 2010; pp 15−54.
(8) Karlsson, R.; Michaelsson, A.; Mattsson, L. *J. Immunol. Methods* **1991**, *145*, 229−40.
(9) Dandliker, W. B.; Levison, S. A. *Immunochemistry* **1968**, *5*, 171−83.
(10) Kapil, M. A.; Herr, A. E. *Anal. Chem.* **2014**, *86*, 2601−2609.
(11) Bordeaux, J.; Welsh, A. W.; Agarwal, S.; Killiam, E.; Baquero, M. T.; Hanna, J. A.; Anagnostou, V. K.; Rimm, D. L. *BioTechniques* **2010**, *48*, 197−209.
(12) Bordeaux, J.; Welsh, A. W.; Agarwal, S.; Killiam, E.; Baquero, M. T.; Hanna, J. A.; Anagnostou, V. K.; Rimm, D. L. *BioTechniques* **2010**, *48*, 197.
(13) Baker, M. *Nature* **2015**, *521*, 274.
(14) Bradbury, A. M.; Plückthun, A. *Nature* **2015**, *520*, 295−295.
(15) Polakiewicz, R. D. *Nature* **2015**, *518*, 483−483.
(16) Freedman, L. P. *Nature* **2015**, *518*, 483−483.
(17) Duncombe, T. A.; Herr, A. E. *Lab Chip* **2013**, *13*, 2115−2123.
(18) Bilgiçer, B. a.; Thomas, S. W.; Shaw, B. F.; Kaufman, G. K.; Krishnamurthy, V. M.; Estroff, L. A.; Yang, J.; Whitesides, G. M. *J. Am. Chem. Soc.* **2009**, *131*, 9361−9367.
(19) Shukla, A. A.; Hubbard, B.; Tressel, T.; Guhan, S.; Low, D. *J. Chromatogr. B: Anal. Technol. Biomed. Life Sci.* **2007**, *848*, 28−39.
(20) Goodrich, J. A.; Kugel, J. F. *Binding and kinetics for molecular biologists*; Cold Spring Harbor Laboratory Press: Cold Spring Harbor, NY, 2007.
(21) Lin, R.; Skandarajah, A.; Gerver, R. E.; Neira, H. D.; Fletcher, D. A.; Herr, A. E. *Lab Chip* **2015**, *15*, 1488−1496.
(22) Hughes, A. J.; Lin, R. K.; Peehl, D. M.; Herr, A. E. *Proc. Natl. Acad. Sci. U. S. A.* **2012**, *109*, 5972−5977.
(23) Hughes, A. J.; Herr, A. E. *Proc. Natl. Acad. Sci. U. S. A.* **2012**, *109*, 21450−21455.
(24) Katsamba, P. S.; Navratilova, I.; Calderon-Cacia, M.; Fan, L.; Thornton, K.; Zhu, M.; Bos, T. V.; Forte, C.; Friend, D.; Laird-Offringa, I.; Tavares, G.; Whatley, J.; Shi, E.; Widom, A.; Lindquist, K. C.; Klakamp, S.; Drake, A.; Bohmann, D.; Roell, M.; Rose, L.; Dorocke, J.; Roth, B.; Luginbuhl, B.; Myszka, D. G. *Anal. Biochem.* **2006**, *352*, 208−21.
(25) Pan, Y.; Duncombe, T. A.; Kellenberger, C. A.; Hammond, M. C.; Herr, A. E. *Anal. Chem.* **2014**, *86*, 10357−10364.
(26) Johnstone, R. W.; Andrew, S. M.; Hogarth, M. P.; Pietersz, G. A.; McKenzie, I. F. C. *Mol. Immunol.* **1990**, *27*, 327−333.
(27) Haynes, W. M. *CRC handbook of chemistry and physics*; CRC Press: Boca Raton, FL, 2013.
(28) Reverberi, R.; Reverberi, L. *Blood Transfus.* **2007**, *5*, 227−240.
(29) Hughes-Jones, N.; Gardner, B.; Telford, R. *Immunology* **1964**, *7*, 72−81.
(30) Karlsson, R.; Falt, A. *J. Immunol. Methods* **1997**, *200*, 121−33.
(31) Moore, B. In *A Seminar on Antigen-antibody Reactions Revisited*; AABB: Arlington VA, 1982; pp 47−66.
(32) Pettersson, K.; Piironen, T.; Seppälä, M.; Liukkonen, L.; Christensson, A.; Matikainen, M.; Suonpää, M.; Lövgren, T.; Lilja, H. *Clin. Chem.* **1995**, *41*, 1480−1488.
(33) Troyer, J. K.; Feng, Q.; Beckett, M. L.; Wright, G. L. In *Urologic Oncology: Seminars and Original Investigations*; Elsevier: New York, 1995; pp 29−37.
(34) Hughes-Jones, N.; Polley, M. J.; Telford, R.; Gardner, B.; Kleinschmidt, G. *Vox Sang.* **1964**, *9*, 385−395.
(35) Hughes-Jones, N.; Gardner, B.; Telford, R. *Biochem. J.* **1962**, *85*, 466.
(36) Hughes-Jones, N.; Gardner, B.; Telford, R. *Biochem. J.* **1963**, *88*, 435.

DOI: 10.1021/acs.analchem.5b04445
Anal. Chem. XXXX, XXX, XXX−XXX